INDIAN JOURNAL OF SCIENCE AND TECHNOLOGY

ORIGINAL ARTICLE

OPEN ACCESS

Received: 21/01/2025

Accepted: 23/04/2025

Published: 14/05/2025

Citation: Shalini Krubha A, Velmurugan S (2025) Pharmacological Applications of Iron Doped Titanium Oxide (Fe/TiO_2) Nanoparticles Derived from *Beta vulgaris* Leaf Extract. Indian Journal of Science and Technology 18(18): 1430-1440. https://doi.org/10.17485/IJST/v18i18.153

* **Corresponding author**.

drvelmuruganphy@gmail.com

Funding: None

Competing Interests: None

Published By Indian Society for Education and Environment (iSee)

ISSN
Print: 0974-6846
Electronic: 0974-5645

Pharmacological Applications of Iron Doped Titanium Oxide (Fe/TiO_2) Nanoparticles Derived from *Beta vulgaris* Leaf Extract

A. Shalini Krubha[1], S. Velmurugan[1,2]*

1 Department of Physics, Annamalai University, Annamalai nagar-608001, Tamil Nadu, India
2 Department of physics, Government Arts College, Chidambaram-608102, Tamil Nadu, India

Abstract

Objectives: To evaluate the structural, morphological and pharmacological application of green synthesized iron doped titanium oxide nanoparticles derived from *Beta vulgaris* leaves extract. **Methods:** A green synthesis of Fe doped TiO_2 a nanoparticle (Fe/TiO_2) was achieved using aqueous extract of *Beta vulgaris* leaves. The obtained Fe/TiO_2 was categorized by analytical techniques including UV, FTIR, XRD, SEM, EDS and TEM. Antibacterial and antifungal activities were analyzed by PDA agar disc diffusion method, while the anticancer studies were carried out using MCF-7 cell-line by MTT assay method. **Findings**: The FTIR spectrum haves showed a new broad band at 574 cm^{-1} indicating to TiO_2 with ferrous ion. The UV spectrum shows absorption peaks at 277.40, 396.30 and 453.30 nm, which tallies with the wavelength of the surface plasmon resonance (SPR) of Fe/TiO_2 bimetallic NPs. The XRD peaks corresponding to rutile phase also emerged at 2θ = 25.61(121) and 39.69 (004) diffraction corresponding to the Fe^{3+} ions could substitute Ti^{4+} from some of the lattice sites of TiO_2. SEM, EDS and TEM images have showed very clear shapes of ferrous ion anatase, Antibacterial activity of green synthesized Fe/TiO_2 has excellent zone of inhibition (14 mm) which is appreciable. Anticancer activities have showed significant effects (IC_{50}= 62.5 μg/m.L). **Novelty:** The nanoparticles of Fe/TiO_2 mediated by *Beta vulgaris* have acted as effective bioreductant and also as potential anticancer agent.

Keywords: Green synthesis; *Beta vulgaris*; Fe/TiO_2NPs; Antimicrobial; Antioxidant; Anticancer activity

1 Introduction

Currently, there is a growing interest for the development and use of nanomaterials in various products and technologies. In the last decade, nanoparticles (NPs) have been deployed in the field of biomedical sciences for targeted delivery of drug, imaging, diagnosis and treatment of diseases and development of antimicrobials[(1)]. Metal and metal-oxide nanoparticles demonstrate novel physico-chemical properties that are not associated with individual or bulk molecules. Among NPs, Titanium oxides (TiO2) NPs validate unique surface chemistry, morphologies and have been used mainly in textile, paper, cosmetics and food industries. Most of the TiO_2 NPs are synthesized using physico-chemical methods that oblige high temperature with pressure and noxious chemicals which make them unbefitting for use as medicine and other biomedical application. Hence the emphasis has shifted to the use of eco-friendly and cost-effective slants to synthesize nano sized TiO_2 particles. One such method of synthesis employs plant extracts as reducing agent. Moreover, this green synthesis approach yields NPs with better morphology and stability[(2)]. Recently, TiO_2-NPs have been synthesized from a range of plants including *Nigella sativa* seed extraction[(3)], aqueous extract of *Catharanthus roseus* (leaf)[(4)], *Eclipta prostrata* aqueous leaf extract[(5)], *Azadirchta indica*[(6)] for various applications. Further, the novel metal doping of TiO_2 improves the efficiency of NPs by manipulating the band gap energy. Amongst NPs, Ag/TiO_2 NPs have been previously synthesized using the extracts of *Citrus limon* and *Nephelium lappaceum* and reported for improved photocatalytic activity[(7)-(8)]. Yet, inadequate reports have appeared apropos green synthesis of Fe/TiO_2-NPs using plant extracts as biological reductants. Owing to the limited information on the usage of plant extracts for synthesizing in FeTiO_2-NPs were synthesized using extract of *Beta vulgaris* using a cost effective and eco-friendly approach. Further, these NPs were characterized employing XRD, SEM, EDS, TEM and UV, FTIR spectroscopic techniques. In the present study, we synthesized the *Beta vulgaris* leaves extract capped Fe/TiO_2 nanoparticle by using bacteria, fungi, antioxidant and investigated their anticancer activity against breast cancer (MCF-7) cell line. *Beta vulgaris L* contain good source of vitamin A, vitamin C, and calcium. The *B. vulgaris* leaves extract has various health benefits such as anticancer, antioxidant, and anti-inflammatory, along with improvement of cardiovascular health with reduction of blood pressure.

2 Methodology

2.1 Collection of materials

The leaves of *Beta vulgaris* were collected from local vegetable market of Chidambaram, Cuddalore district, Tamil Nadu, India.

2.2 Preparation of extract *Beta vulgaris*

The laves of *Beta vulgaris* were cleaned with water for 3 times and followed by deionized water to clean the dust; plant leaves were sheltered, dried totally for 7 days to drain out moisture and then ground to powder. The 10 g of powdered sample was added to 50 ml of double distilled water (DDW) and left for incubation and intermittent stirring was done. Sample was boiled for one hour, cooled to room temperature and filtered using Whatman1$\neq$ filter paper, and filtrate used for the synthesis of iron doped TiO_2-NPs.

2.3 Green synthesis of iron doped TiO_2 nanoparticles (Fe/TiO_2)

Fe/TiO_2 NPs were synthesized using iron nitrate, titanium isopropoxide and leaves extract of *Beta vulgaris*. In short, 20 mM titanium isopropoxide was added drop wise into 50 ml absolute ethanol, stirred vigorously for 20 min at room temperature and after that few drops of 65% HNO_3 was added. *Beta vulgaris* leaves extract (5 mL) and 1 mM of iron nitrate ($Fe(NO_3)_2$) were added to the previously prepared mixture and stirred for 1 hr. Subsequently, deionized water was added to the mixture and the consequent solution was shaken for couple of hours at room temperature (RT) for the gel formation, this gel was kept for 1 day at RT. After drying at 80°C for 1 day, the as-prepared *Beta vulgaris* extract and Fe/TiO_2 samples were obtained and then annealed at 400°C for 3 h to give a pale reddish material.

2.4 Characterization of spherical Fe/TiO_2 NPs

The UV-Vis absorption studies were conducted on UV spectrophotometer (Thermo Scientific EVOLUTION-600). FT-IR analysis was carried out on a Perkin Elmer FTIR spectrophotometer spectrum two (Perkin Elmer Life and Analytical Sciences, CT, USA). Endorsement of crystal phases and determination of average crystalline size was performed using powder XRD (X-ray diffraction). Diffractions dimensions were achieved through PAN analytical PW 3040/60 X'Pert PRO instrument using Ni-filtered Cu-Ka radiation (1.54 Å) curve fitting and integration was used for X'Pert high score plus software. The FESEM (Filed Emission Scanning Electron Microscopy) was done to study the morphology and elements identification were done by EDS (Energy Dispersion Spectroscopy) on JEOL JEM-2300, of the NPs. TEM (Transmission Electron Microscopy) gave the size and SAED (selective area electron diffraction) pattern at a voltage of 200 kV on JEOL JEM-1200EX (Japan).

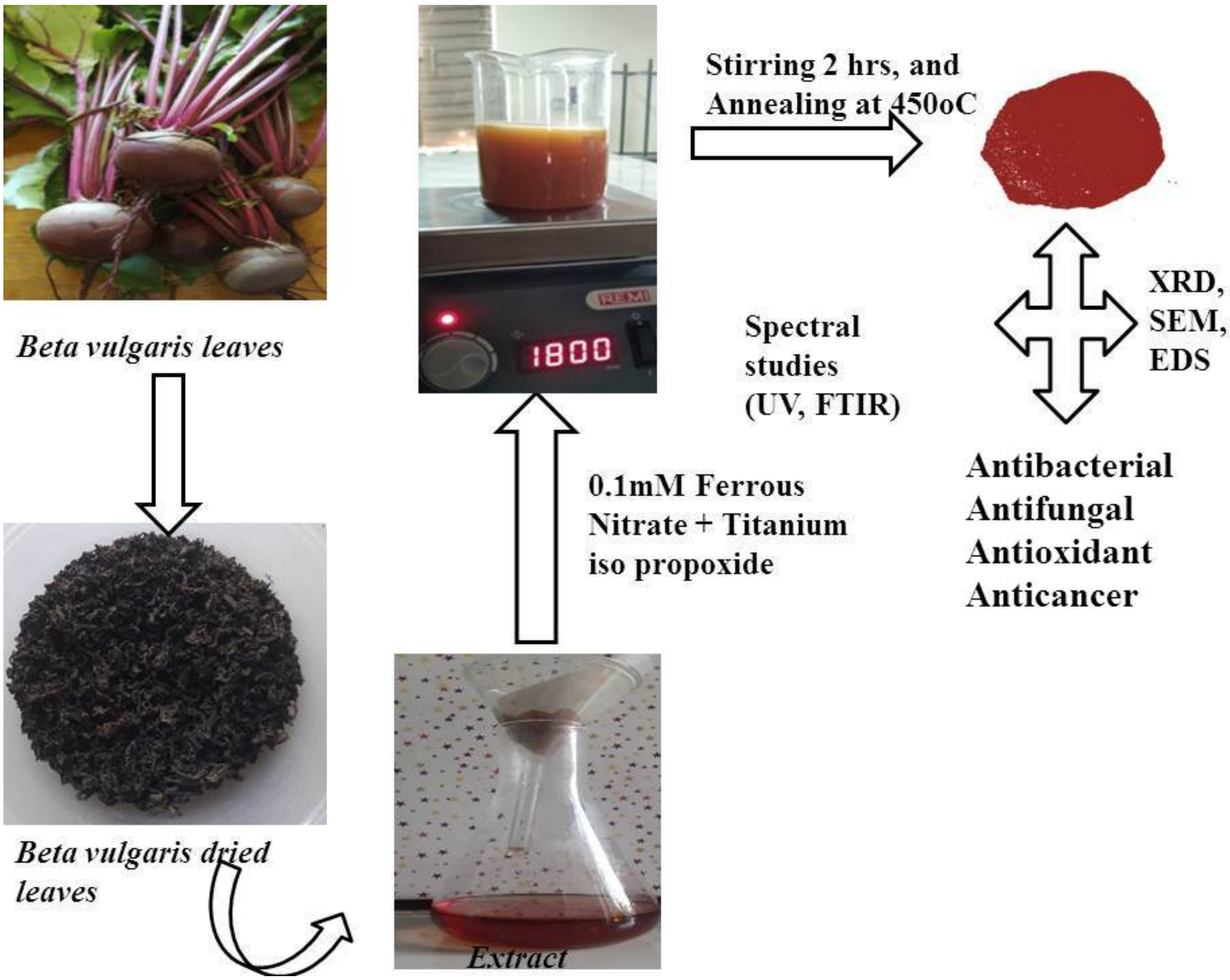

Fig 1. Scheme of Green synthesis of Fe/TiO_2 NPs by *Beta vulgaris*

2.5 Antimicrobial studies

Disc diffusion method was used for antibacterial and antifungal assays to evaluate the antimicrobial potential of synthesized Fe/TiO_2NPs by *Beta vulgaris*.

2.5.1. Antibacterial assay

Four pathogenic bacterial strains, two gram positive (*Staphylococcus aureus*-ATCC 12600, *Escherichia coli*-ATCC 2592,) and two gram negative (*Pseudomonas aeruginosa*-ATCC 15442), *Bacillus cereus*-ATCC 14579) were used in this assay. Bactericidal activity was determined by using disc diffusion method as described by Sheikh et al.[9]. Bacterial cultures were refreshed in nutrient broth for 24 h at 37°C. Nutrient agar medium was used for the growth of bacterial strains. Filter paper discs of 6 mm in size ware prepared from whatman no. 1 filter paper. Media, filter paper discs along with other apparatus required in this assay were autoclaved for sterilization and experiment was performed in microbiological safety cabinet. Bacterial strains were streaked on solidified labeled nutrient agar plates. Ampicillin was used as standard drug. Then 20 mg of samples were loaded per disc, placed on respective places in petri plate and incubated for 24 h at 37°C for antibacterial activity. Zones of inhibitions were measured after 24 h.

2.5.2. Antifungal assay

Fungicidal activity of synthesized Fe/TiO_2NPs by *Beta vulgaris* were unhurried by discerning the growth response of two fungal strains (*Candida albicans*- ATCC 10231, *Trichoderma viride*- QM 3090). PDA broth was used for energizing fungal culture and grown on potato dextrose agar (PDA). Slight modified method of Sheikh et al.[9] was followed for measuring the fungicidal capacities. All apparatus were autoclaved for sterilization. Experiment was performed in triplicate and carried out in microbiological safety cabinet. Sample solution was absorbed on discs and placed on respective labeled solidified SDA plates. Amphotericin B was used as standard drug and 20 mg per disc of nanoparticles was used for antifungal activity. Plates were incubated for 24 h at 28° C and measured the zone of inhibition.

2.6 Antioxidant studies by DPPH method

Antioxidant potential of Fe/TiO_2 NPs against DPPH was determined using method described by Mahendra et al.,[10] with slight modification. DPPH assay was performed in 96 wells plate. Test sample (20 ml) from stock solution was poured in respective well of plate and then 180 ml of DPPH solution was added in each well to make 200 ml final volume. Ascorbic acid was used as reference standard. Mixture was incubated at room temperature for half an hour. Change in color from violet to yellow was observed due to the antioxidation potential. Absorbance of reaction mixture was measured at 517 nm on microplate reader. Scavenging activity was calculated by given equation.

$$\%Scavenging = \frac{OD\,of\,control - OD\,of\,test\,sample}{OD\,of\,control}$$

OD = optical density absorbance

2.7 Anticancer study by MTT assay

Anticancer effect of the green synthesized Fe/TiO_2NPs was determined using MTT assay. Momentarily, 1x10^3 cells were plated and permissible to observe in 96-well plate under anaerobic conditions as described previously. Post incubation, 10-mL of MTT solution was added in each well to make incubation for 4-hours in a CO_2 incubator. Afterward, 200 mL of DMSO was added to each well after retreat supernatant[11]-[12]. The development of the color was read at 550 nm. MCF-7 cell line was obtained from National Centre for Cell Sciences, Pune (NCCS). The cells were kept in DMEM augmented with 10% FBS, penicillin (100 U/ml), and streptomycin (100 μg/ml) in a humidified atmosphere of 50 μg/ml CO_2 at 37°C. Cells (1×10^5/well) were plated in 24-well plates and incubated in 37^0C with 5% CO_2 condition. After the cell reaches the confluence, the several concentrations of the samples were added and incubated for 24hrs. After incubation, the sample was removed from the well and washed with phosphate-buffered saline (pH 7.4) or DMEM without serum. 100μl/well (5mg/ml) of 0.5% 3-(4,5-dimethyl-2-thiazolyl)-2, 5-diphenyl–tetrazolium bromide (MTT) was added and incubated for 4 hours. After incubation, 1ml of DMSO was added in all the wells. The absorbance at 570nm was measured with UV-Spectrophotometer using DMSO as the blank. Measurements were performed and the concentration required for a 50% inhibition (IC_{50}) was determined graphically. The % cell viability was calculated using the following formula

$$\%Cell\,viability = \frac{A\,570\,of\,treated\,cells}{A\,570\,of\,control\,cells} \times 100$$

Graphs are plotted using the % of Cell Viability at Y-axis and concentration of the sample in X-axis. Cell control and sample control is included in each assay to compare the full cell viability assessments.

3 Results and Discussion

3.1 FTIR Spectral analysis

The FTIR Spectrum (Figure 2a) of *Beta vulgaris* leaf extract indicated characteristic signals at 3373, 1673, 1384, 1113 and 618 The wide bands observed at 3373 cm^{-1} indicates alcoholic (-O-H) stretching vibrations, sharp medium peaks at 1643 cm^{-1} have represented in –C=O stretching vibration, this carbonyl functional groups have represented in *Beta vulgaris* leaf extract have present in various carbonyl groups like aldehyde, acids, esters, ketones etc.. The weak peaks at 1383 cm^{-1} have shown in bending deformation peaks of methyl, and methylene groups, the strong peaks at 1113 cm^{-1} have shown in bending vibrations of C-C-C bonding, the sharp peaks have shown in the bending vibration at 618cm^{-1} indicates C-H deformations. The FTIR Spectrum of Fe/TiO_2 nanoparticles indicated characteristic signals at 3424, 2027, 1630, 1392, 1271, 1017 and 574 IR range of nanoparticles, a shift in the absorbance tops was watched a solid expansive band at 3424 cm^{-1} could be credited to the extending vibration of the hydroxyl gathering and the interlayer water molecules[13]. This marvel was essentially brought about through Ti-O-H extending vibration. The sharp peaks at 2027 have shown C≡C (symmetry reduces intensity). Very sharp band at 1630 cm^{-1}

with much reduced intensity compared with extract, this peak assigned carbonyl and twisting the vibration of H-O-H bond on TiO_2 catalyst [14] and at 1392 cm^{-1} proposing the official of Fe-O-Ti individually. Another sharp peak obtained at 1271 cm^{-1} have reveals that C(O)–O stretching vibrations and –OH in plane vibration, The weak band observed at 1017 cm^{-1} reveals that in bending vibrations of C-C-C bonding. The band centered at 574 cm^{-1} was due to metal–oxygen, i.e., Ti–O and Fe–O, bonds

3.2 UV-visible Spectral analysis

The *Beta vulgaris* leaf extract, phytosynthesized Fe/TiO_2 bimetallic NPs solution were subjected to UV-visible spectroscopy, in order to shed light on the mechanism of Fe/TiO_2 bimetallic NPs formation [15]. The recorded spectra have shown in Figure 2c. The spectra chronicled absorption peak between the regions from 200 to 850 nm, while the recorded spectra during the reduction showed absorption peaks at 277.40, 396.30 and 453.30 nm, which corresponds to the wavelength of the surface plasmon resonance (SPR) of Fe/TiO_2 bimetallic NPs. The Fe/TiO_2 bimetallic NPs showed a absorption peak at 277.40 nm, which is a good agreement with the bimetallic NPs (Fe:Ti) 1:1 ratio onwards.

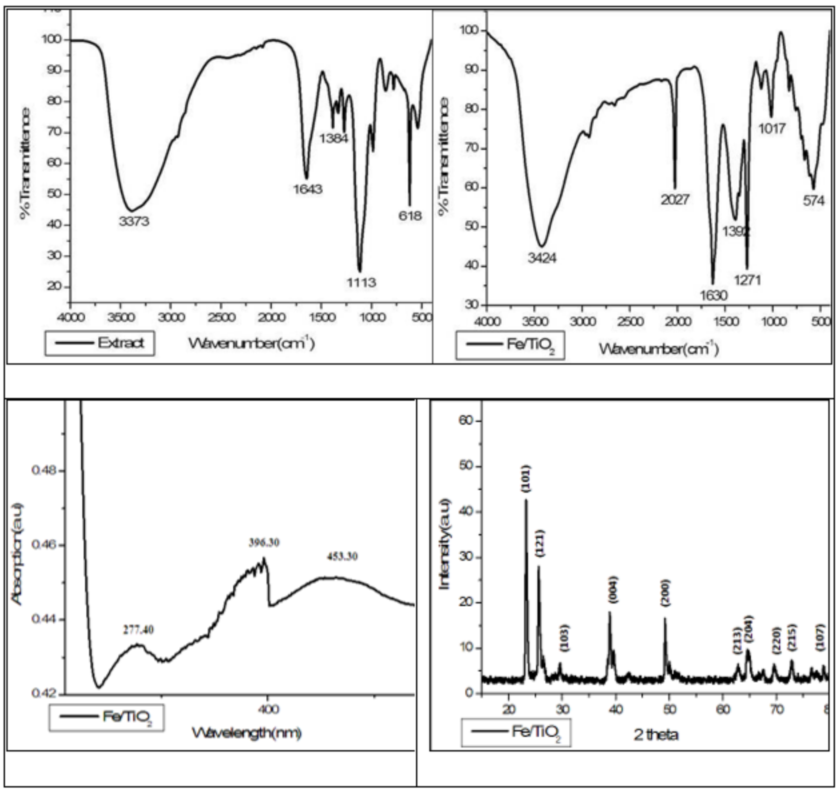

Fig 2. (a) FTIR spectrum of *Beta vulgaris* leaf extract, (b) FTIR Spectrum of Fe/TiO_2NPs mediated by *Beta vulgaris* leaf extract, (c) UV Spectrum, (d) XRD spectrum of Fe/TiO_2NPs mediated by *Beta vulgaris* leaf extract

3.3 Powder XRD analysis

Figure 2d present the XRD diffraction patterns of Fe-doped-TiO_2 nanoparticles. The XRD studies clearly demonstrated the presence of both anatase and rutile phases with anatase as the major phase. The presence of main diffraction peaks in the XRD pattern of Fe-doped-TiO_2 nanoparticles at 2θ = 23.28°, 25.61°, 29.63°, 39.69°, 49.21°, 62.86°, 64.57°, 69.40°, 73.01° & 79.04° are allocated for (101), (121), (103), (004), (200), (213), (204), (220), (215) & (107) lattice planes of anatase phase (JCPDS No. 21-1272). The XRD peaks corresponding to rutile phase also emerged at 2θ = 25.61 and 39.69 diffraction angles corresponding to (121) and (004) diffraction planes [16]. The synthesized samples did not exhibit any diffraction peaks for Fe, which suggests that the Fe^{3+} content in the Fe doped TiO_2 was below the detection limit, and due to almost similar ionic radii, the Fe^{3+} ions could substitute Ti^{4+} from some of the lattice sites of TiO_2. This further indicates that Fe^{3+} ions were successfully integrated into TiO_2 matrix homogeneously without the development of iron oxide on the TiO_2 surface. This homogeneous distribution of Fe^{3+} ions in TiO_2 matrix and low concentration, responsible for the absence of any Fe^{3+} peaks in the XRD patterns, have also been reported earlier in the literature (17) - (18). The average crystallite size of the synthesized nanoparticles was estimated using the Scherrer formula (**Equation (1)**) and was found to be around 14 nm.

$$d = \frac{0.89\lambda}{\beta \cos\theta} \tag{1}$$

Where $\lambda = 1.542\text{Å}$, θ = Bragg angle of diffraction, β = full width at half maximum.

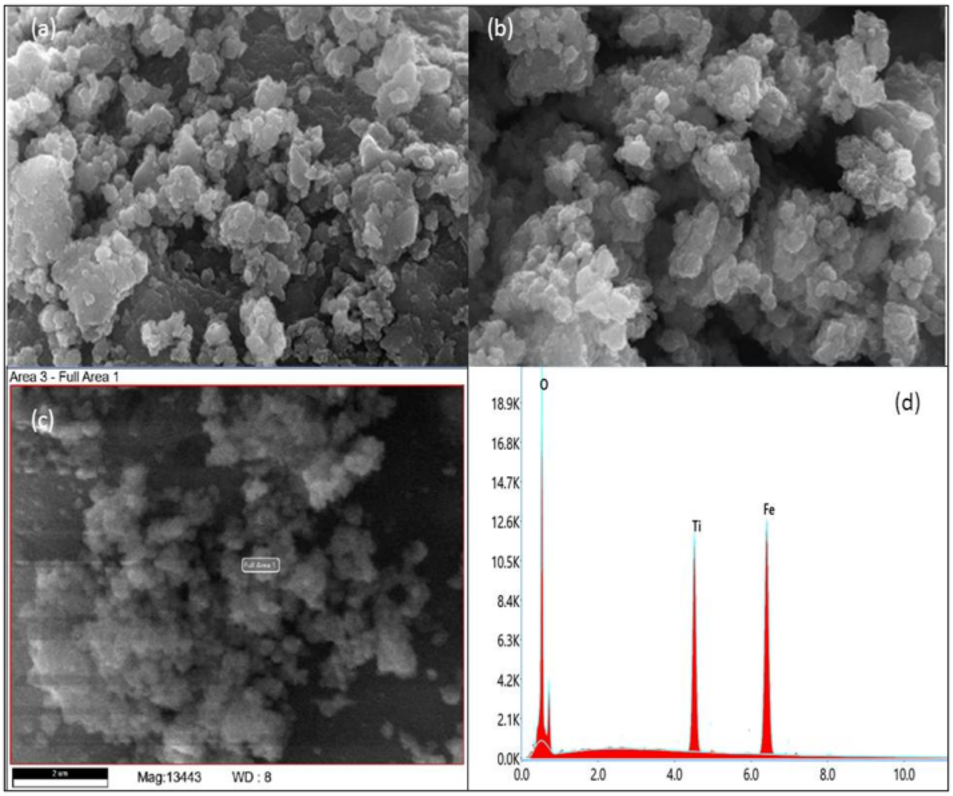

Fig 3. (a) and (b) SEM Image of Fe/TiO_2 NPs, (c) EDS-Micrographs image of Fe/TiO_2 NPs, (d) EDS Spectrum of Fe/TiO_2 mediated by *Beta vulgaris* leaf extract

3.4 SEM with EDS Analysis

Surface morphology was determined with SEM. The amalgamated Fe/TiO_2 were disseminated haphazardly having jagged surface (Figure 3a & b). Synthesized NPs were circular in shape with an average size of 24.25 nm. However, larger particles of Fe/TiO_2 were also noticed perchance due to the accretion of NPs during the preparation of samples. Chemical composition of synthesized NPs was unwavering with EDS Micrographs image (Figure 3c). EDS spectrum shows (Figure 3d) presence of Ti & Fe peaks around 4.5 eV and 6.4 eV, respectively. EDS spectrum analysis also publicized that iron is in metallic form and free from scums.

3.5 TEM Analysis

TEM pictures demonstrated the presence of polycrystalline Fe/TiO_2 NPs with *Beta vulgaris* leaves extract (Figure 4a-c). The biosynthesized Fe/TiO_2 nanoparticles were predominately globular in shape with an average size of 0.5–50 nm and some were agglomerated skimpy a resilient interaction with the molecules of *Beta vulgaris* leaves extract. SAED pattern exhibits discrete circular diffraction rings corresponding to anatase phase (Figure 4d). Obtained polycrystalline diversion rings of fictional spherical NPs were in agreement with the earlier study.

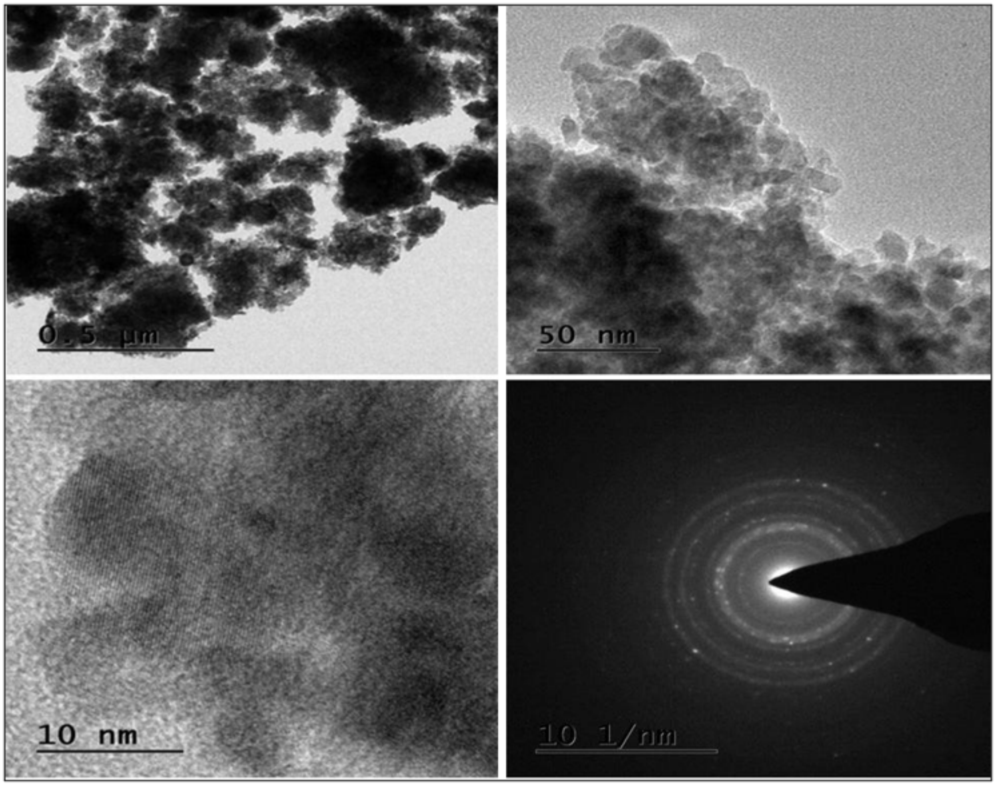

Fig 4. (a), (b) and (c) TEM Image of Fe/TiO_2 NPs, (d) SAED pattern of Fe/TiO_2 mediated by *Beta vulgaris* leaf extract

3.6 Antimicrobial studies

3.6.1. Antibacterial Activity

Antibacterial accomplishments of synthesized Fe/TiO_2-NPS have shown in Figure 5, were studied amongst both (Gram positive and Gram negative) pathogenic bacteria. Fe/TiO_2 NPs showed maximum zone of inhibition against *P. aeruginosa* (18 mm) at 1000 μg/ml concentration and *B. cereus* (11 mm) at 1000 μg/ml and 750 μg/ml, these two pathogens shown outstanding activity compared with standard drugs. Antibacterial activities of *E. coli* have shown in perpetual zone of inhibition (9 mm) for three concentrated test solutions (1000 μg/ml, 750 μg/ml and 500 μg/ml). Fe/TiO_2 NPs showed maximum zone of inhibition against *S. aureus* (9mm) at 1000 mg/ml concentration, other two concentrations such as 750 mg/ml, 500 mg/ml have shown in same zone of inhibition (8mm). Antibiotics were used as positive control[19]. The Antimicrobial activity of Fe/TiO_2-NPs is generally endorsed to disrupting membrane integrity by reactive oxygen species (ROS) leading for phospholipid peroxidation and ultimately leads to cell death.

3.6.2. Antifungal activity

Antifungal activities of synthesized Fe/TiO_2-NPs by *Beta vulgaris* leaves extract have shown in Figure 5, were studied by fungal strains such as *Candida albicans, Trichoderma viride.*

Fe/TiO_2 NPs showed maximum zone of inhibition against *Candida albicans* (12 mm) at 1000 μg/ml concentration, the antifungal activity of Fe/TiO_2 against *C. albicans* have shown the concentration of test solution increases, antifungal activity also increases, 10 mm at 750 μg/ml and 9mm at 500 μg/ml[20]. Antifungal activities of synthesized Fe/TiO_2-NPs have shown constant zone of inhibition (9 mm) at three concentrations of the test solutions (1000 μg/ml, 750 μg/ml, 500 μg/ml).

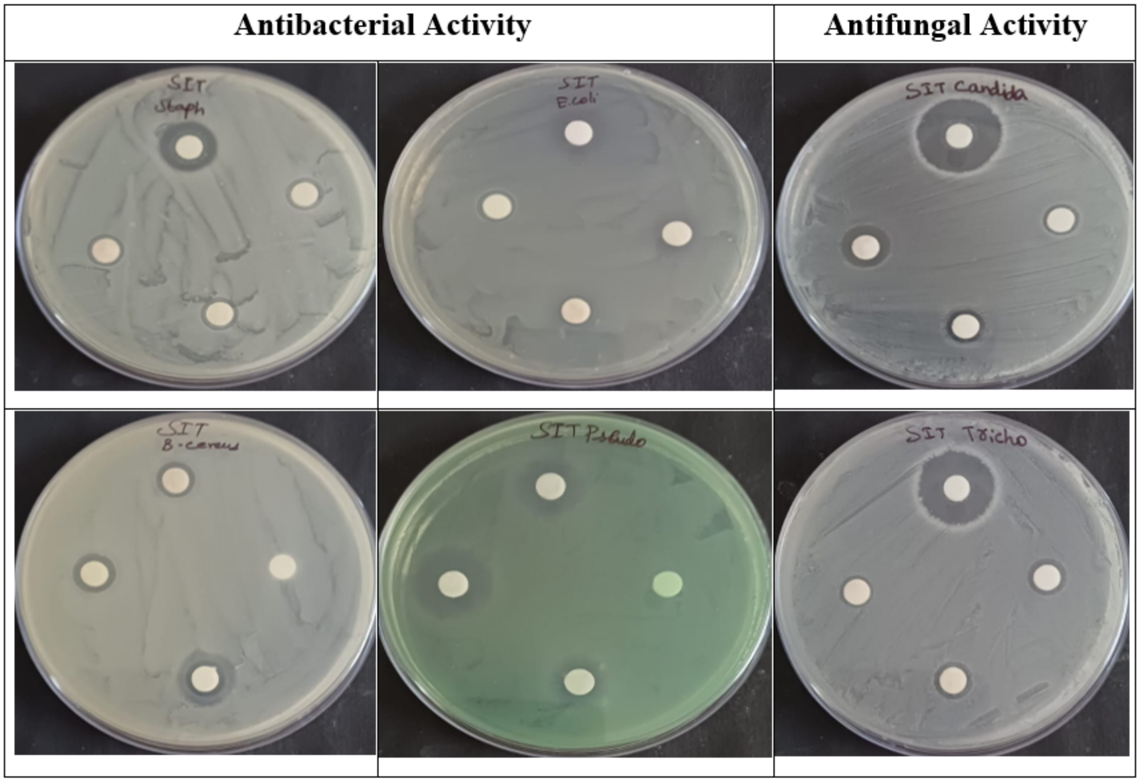

Fig 5. Antibacterial and antifungal activity of Fe/TiO_2-NPs by *Beta vulgaris* leaves extract

Table 1. Zone of inhibition values of Antibacterial and Antifungal activity of Fe/TiO_2-NPs by *Beta vulgaris* leaves extract

Organisms		**Zone of Inhibition (mm)**			
		Sample (μg/ml)			**Standard**
		1000	750	500	
Antibacterial organism	*Staphylococcus aureus*	9	8	8	13
	Escherichia coli	9	9	9	13
	Pseudomonas aeruginosa	18	13	-	14
	Bacillus cereus	11	11	-	10
Antifungal organism	*Candida albicans*	12	10	9	20
	Trichoderma viride	9	9	9	20

3.7 Antioxidant Activity

The DPPH assay is widely used for screening antioxidant activity because it is sensitive enough to detect active compounds at low concentrations[(21)]. DPPH is a nitrogen-centered free radical, and hence any compound that scavenges significant amounts of DPPH could reduce levels of other reactive nitrogen species in living cells.

From the results, the biologically synthesized Fe/TiO_2-NPs *Beta vulgaris* leaves extract appeased DPPH free radicals noticeably and dose-dependently (200 μg/ml, 400 μg/ml, 600 μg/ml, 800 μg/ml and 1000 μg/ml) (Figure 6). However, this activity was much lower than that of the BHA standard. BHA is a pure antioxidant standard whose mechanism of exploit is precisely known. Fe/TiO_2-NPs however have no known mechanism of action as an antioxidant as this is one of the earliest reports on its antioxidant effect on DPPH free radicals[(22)]. Hence, reason for its relatively lower antioxidant activity compared to DPPH cannot be adequately explained.

Table 2. Antioxidant activity of Fe/TiO_2-NPs by *Beta vulgaris* leaves extract

S.NO	Concentration (μg/ml)	DPPH %
1	200	34.17
2	400	45.05
3	600	53.6
4	800	64.32
5	1000	79.22

It is therefore expedient to conducted further research into the mechanism of action of Fe/TiO_2-NPs in scavenging DPPH free radicals.

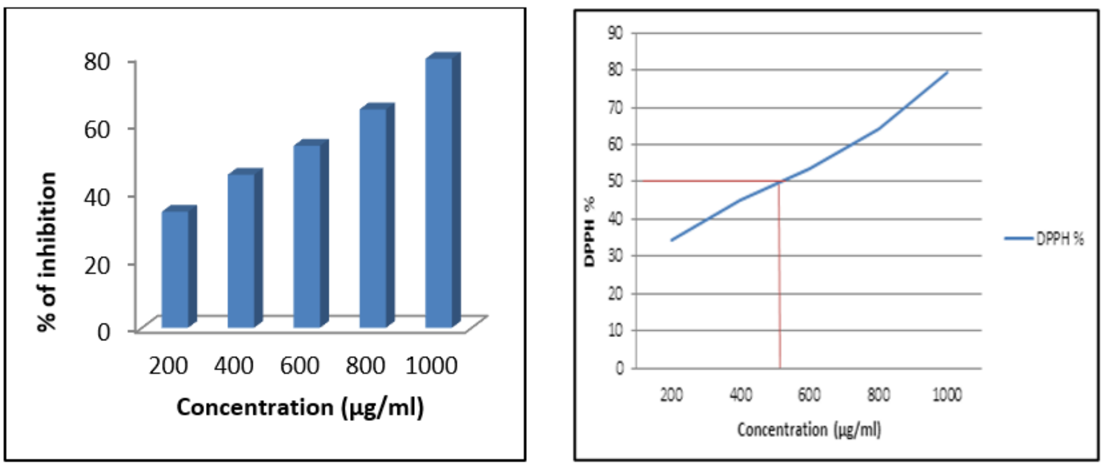

Fig 6. Antioxidant activity of Fe/TiO_2-NPs by *Beta vulgaris* leaves extract

3.8 Anticancer Activity

Anticancer action of the Fe/TiO_2-NPs was studied against the MCF-7 cell line by MTT assay. These effects on cancerous cell were studied at different concentrations (7.8 μg/mL,15.6 μg/mL,31.2 μg/mL,62.5 μg/mL,125 μg/mL, 250 μg/mL, 500 μg/mL, 1000 μg/mL). IC_{50} of *Beta vulgaris* leaves extract Fe/TiO_2-NPs observed at conc. of 62.5 μg/m.L against MCF-7 cell line. The bar diagram of efficacy of biosynthesized Fe/TiO_2-NPs against MCF-7 cell line at different concentration (Figure 7).

The lowest inhibitory action was observed from a concentration of 250 μg/ml. In this report, the anticancer activity was observed and that the synthesized Fe/TiO_2 nanoparticles were a dose dependent inhibition activity against human breast cancer cells [(23)]-[(24)]. Some of the approved chemotherapeutic agents caused side effects and high costs. Therefore, there is an important need to develop unconventional medicines against this deadly disease. Synthesized iron doped titanium oxide nanoparticles to fulfill the need for new therapeutic treatments were discovered.

The Fe/TiO_2 nanoparticles are having the good results against MCF-7 lines in that 31.2 μg/ml show fine results shows by 125, 250, 500 and 1000 μg/ml.

4 Conclusion

The present study achieved the synthesis of Fe/TiO_2-NPs nanoparticles using biological agent, which is eco-friendly, of low cost and capable of fabricating at room temperature. The present study, *Beta vulgaris* leaves extract phytochemicals acts as both reducing and stabilizing agents. The NPs were characterized by UV–vis, FTIR, XRD, SEM, EDS analysis. The UV–vis spectra confirm the formation of green synthesized Fe/TiO_2-NPs based on surface plasmon resonance study. The phytochemicals were responsible for reducing and capping of Fe/TiO_2-NPs, which was confirmed by FTIR spectral datas. The EDS results determined the elemental analysis, SEM and TEM results revealed uniform anatase phase with ferrous ion containing Fe/TiO_2-NPs. The *Beta vulgaris* synthesized Fe/TiO_2-NPs were potent in inhibiting *P.aeruginosa* and thus can be an excellent antibacterial agent.

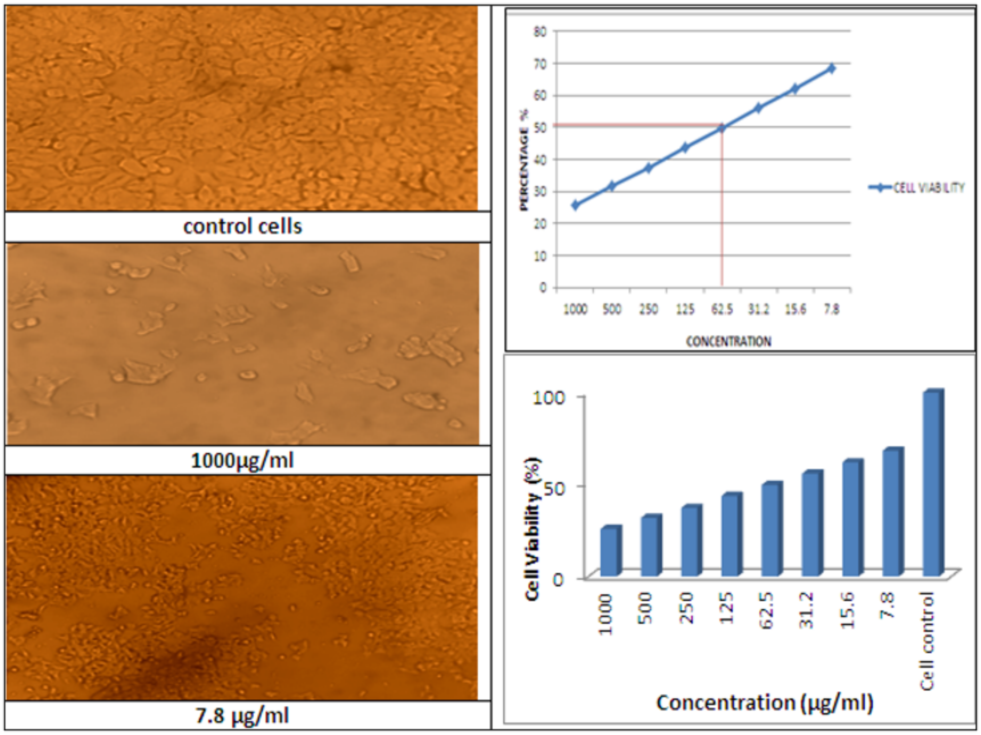

Fig 7. Anticancer activity of Fe/TiO_2-NPs with MCF-7 cell line by *Beta vulgaris* leaves extract

Table 3. Anticancer activity of Fe/TiO_2-NPs by *Beta vulgaris* leaves extract

S. No	Concentration (μg/ml)	Cell Viability (%)
1	1000	25.92
2	500	31.90
3	250	37.32
4	125	43.87
5	62.5	49.85
6	31.2	55.98
7	15.6	62.10
8	7.8	68.37
9	Cell control	100

Fe/TiO_2-NPs have shown poor antifungal effect with both the fungal strains. Fe/TiO_2-NPs have shown excellent antioxidant activity was indicating the half of the minimum inhibitory concentration values (IC_{50}=510 μg/ml). The biosynthesized metal nanoparticles & *Beta vulgaris* leaves extract showed promising anticancer activity with MCF-7 cell line. The outcome of the results confirms that the leaf phytochemicals of *Beta vulgaris* are responsible for formation of Fe/TiO_2-NPs and exhibited potent biological activity tried.

5 Conflicts of interest

The authors declare no conflict of interest.

References

1) Pillai AM, Harisankar A, Salini PS. Green synthesis of TiO2 nanoparticles using Beta vulgaris extract and the evaluation of their photocatalytic and antibacterial activity. *Ionics*. 2024;30:4257–4270. https://doi.org/10.1007/s11581-024-05577-3.

2) Nazifa TT, Nushrat F, R MMH, Salman SM. The Promise of Metal-Doped Iron Oxide Nanoparticles as Antimicrobial Agent. *ACS Omega*. 2024;9:16–32. Available from: https://pubs.acs.org/doi/epdf/10.1021/acsomega.3c06323?ref=article_openPDF. https://doi.org/10.1021/acsomega.3c06323.
3) Ramya R, Muthulakshmi G, Sudhahar S, Bhaskaran A. Green synthesis and characterization studies of TiO2 nanoparticles and its potential biological performance. *Nano-Structures & Nano-Objects*. 2024;39:101322. https://doi.org/10.1016/j.nanoso.2024.101322.
4) Ansari FS, Daneshjou S. Optimizing the green synthesis of antibacterial TiO2 - anatase phase nanoparticles derived from spinach leaf extract. *Scientific Reports*. 2024;14:22440. https://doi.org/10.1038/s41598-024-73344-5.
5) Jitha NG, Deepa K, Ayana N. Enhanced Viability of Iron-Doped Titanium Dioxide Nanoparticles with Antibacterial Efficacy. *Brazilian Journal of Physics*. 2025;55:70. https://doi.org/10.1007/s13538-025-01702-3.
6) Ansari FS, Daneshjou S. Optimizing the green synthesis of antibacterial TiO2 - anatase phase nanoparticles derived from spinach leaf extract. *Scientific Reports*. 2024;14(1):22440. https://doi.org/10.1038/s41598-024-73344-5.
7) Alzahrani A. A study of the anticancer potential of Pluronic F-127 encapsulated Fe2O3 nanoparticles derived from Berberis vulgaris extract. *Green Processing and Synthesis*. 2023;12(1):20230126. https://doi.org/10.1515/gps-2023-0126.
8) Mohd HM, Tarun KU, Fahad K, Pratibha P, Moon NP, Amit BS, et al. Metallic and metal oxide-derived nanohybrid as a tool for biomedical applications. *Biomedicine & Pharmacotherapy*. 2022;155:113791. https://doi.org/10.1016/j.biopha.2022.113791.
9) Sheikh M, Makkad S, Shende S, Deshmukh M. Antimicrobial Efficacy of Metal-Doped Titanium Dioxide Nanoparticles: A Comprehensive Review. *International Journal of Pharmaceutical Investigation*. 2024;14(4):1042–1051. https://doi.org/10.5530/ijpi.14.4.114.
10) Mahendra SR, Shobhit G, Roopashree R, Komal P, Kamini S, Madhur G, et al. Antibacterial, antifungal, antioxidant and anticancer activities of Sr and Fe doped TiO2 nanomaterial. *Journal of the Indian Chemical Society*. 2025;p. 101587. https://doi.org/10.1016/j.jics.2025.101587.
11) Soad ZA, Mokhtar MMM, Jia HP, Elsayed TH. Improving photocatalytic, anticancer and antioxidant activities of greenly synthesized TiO2 nanoparticles by triple doping (Al, C, S). *Journal of the Taiwan Institute of Chemical Engineers*. 2024;p. 105795. https://doi.org/10.1016/j.jtice.2024.105795.
12) Salve P, Vinchurkar A, Raut R, Chondekar R, Lakkakula J, Roy A, et al. An Evaluation of Antimicrobial, Anticancer, Anti-Inflammatory and Antioxidant Activities of Silver Nanoparticles Synthesized from Leaf Extract of Madhuca longifolia Utilizing Quantitative and Qualitative Methods. *Molecules*. 2022;27:6404. https://doi.org/10.3390/molecules27196404.
13) Ismail MA, Hedhili MN, Anjum DH, Singaravelu V, Chung SH. Synthesis and Characterization of Iron-Doped TiO2 Nanoparticles Using Ferrocene from Flame Spray Pyrolysis. *Catalysts*. 2021;11(4):438. https://doi.org/10.3390/catal11040438.
14) Ramya R, Muthulakshmi G, Sudhahar S, Bhaskaran A. Green synthesis and characterization studies of TiO2 nanoparticles and its potential biological performance. *Nano-Structures & Nano-Objects*. 2024;39:101322. https://doi.org/10.1016/j.nanoso.2024.101322.
15) Remya RR, Angeline J, Hariharan K, Antony VS, Rajalakshmi D, Shobana N, et al. In vitro free radical scavenging effects of Titanium dioxide Nanoparticles (TiO2 NPs) biosynthesized using stem extract of Cissus quadrangularis. *Letters in Applied Nanobioscience*. 2024;13(3):109. https://doi.org/10.33263/LIANBS133.109.
16) Ghareeb A, Fouda A, Kishk RM, Kazzaz WME. Unlocking the potential of titanium dioxide nanoparticles: an insight into green synthesis, optimizations, characterizations, and multifunctional applications. *Microbial Cell Factories*. 2024;23(1):341. https://dx.doi.org/10.1186/s12934-024-02609-5.
17) Ismael M. Enhanced photocatalytic hydrogen production and degradation of organic pollutants from Fe (III) doped TiO2 nanoparticles. *Journal of Environmental Chemical Engineering*. 2020;8:103676. https://dx.doi.org/10.1016/j.jece.2020.103676.
18) Archana R, Saurabh P, Kapil K, Anjali K, Samridhi C, Mahesh K, et al. Multifaceted properties of TiO2 nanoparticles synthesized using Mangifera indica and Azadirachta indica plant extracts: antimicrobial, antioxidant, and non-linear optical activity investigation for sustainable agricultural applications. *Materials Advances*. 2024;5:2767. https://dx.doi.org/10.1039/d3ma00414g.
19) Ali H, Dixit S, Alarif S. Green synthesis of Titanium dioxide nanoparticle using combination of plants and its antimicrobial study with their characterization. *Materials Research Express*. 2024;11:095403. https://dx.doi.org/10.1088/2053-1591/ad7dd3.
20) Prabhjot SJ, Dapinder K, Ram P, Joginder S. Green synthesis of titanium dioxide nanoparticles: Development and applications. *Journal of Agriculture and Food Research*. 2022;10:100361. https://doi.org/10.1016/j.jafr.2022.100361.
21) Joudeh N, Linke D. Nanoparticle classification, physicochemical properties, characterization, and applications: a comprehensive review for biologists. *Journal of Nanobiotechnology*. 2022;20. https://dx.doi.org/10.1186/s12951-022-01477-8.
22) Umar H, Rizaner N, Usman AG, Aliyu MR, Adun H, Ghali UM. Prediction of Cell Migration in MDA-MB 231 and MCF-7 Human Breast Cancer Cells Treated with Albizia Lebbeck Methanolic Extract Using Multilinear Regression and Artificial Intelligence-Based Models. *Pharmaceuticals*. 2023;16(6). https://dx.doi.org/10.3390/ph16060858.
23) Saravanan M, Vahidi H, Cruz DM, Vernet-Crua A, Mostafavi E, Stelmach R. Emerging Antineoplastic Biogenic Gold Nanomaterials for Breast Cancer Therapeutics: A Systematic Review. *International Journal of Nanomedicine*. 2020;15:3577–3595. https://doi.org/10.2147/IJN.S240293.
24) Eslamiehei FM, Mashreghi M, Matin MM. Advancing colorectal cancer therapy with biosynthesized cobalt oxide nanoparticles: a study on their antioxidant, antibacterial, and anticancer efficacy. *Cancer Nanotechnology*. 2024;15(1). https://dx.doi.org/10.1186/s12645-024-00258-2.